

~~CONFIDENTIAL~~

Copy  
RM L56C15

03



UNCLASSIFIED



# RESEARCH MEMORANDUM

SOME NOTES ON THE VIOLENT LATERAL-LONGITUDINAL  
COUPLING MOTIONS OF THE DOUGLAS X-3

AIRPLANE IN AILERON ROLLS

By Ralph W. Stone, Jr.

Langley Aeronautical Laboratory  
Langley Field, Va.

*Handwritten notes:*  
7/17/56  
956  
NACA  
AA-129  
Effective  
Authority

CLASSIFIED DOCUMENT

This material contains information affecting the National Defense of the United States within the meaning of the espionage laws, Title 18, U.S.C., Secs. 793 and 794, the transmission or revelation of which in any manner to an unauthorized person is prohibited by law.

## NATIONAL ADVISORY COMMITTEE FOR AERONAUTICS

WASHINGTON

May 17, 1956

~~CONFIDENTIAL~~

15  
NACA H

UNCLASSIFIED

## NATIONAL ADVISORY COMMITTEE FOR AERONAUTICS

## RESEARCH MEMORANDUM

SOME NOTES ON THE VIOLENT LATERAL-LONGITUDINAL  
COUPLING MOTIONS OF THE DOUGLAS X-3

## AIRPLANE IN AILERON ROLLS

By Ralph W. Stone, Jr.

## SUMMARY

Recent flight experiences on the Douglas X-3 airplane and other contemporary designs, which have their mass concentrated primarily along the fuselage (moment of inertia about Z body axis much larger than moment of inertia about X body axis), have indicated that large violent coupled motions exist on such airplanes. Analytical studies of such motions have been made to evaluate the nature and cause of these motions. The results of a rather limited study of the X-3 motions are included herein.

The results indicate that the violent lateral-longitudinal coupling motions encountered on the X-3 were apparently caused by the inclination of the principal axis below the flight path at the onset of the rolling maneuvers and the existence of a value of pitching moment due to sideslip possibly combined with a trim change near Mach number 1. The inclination of the principal axis below the flight path caused the sideslip to be positive in left rolls which, in turn, created a rolling moment due to dihedral effectiveness which helped to increase the rolling velocity to critical values. The pitching moment due to sideslip was such as to cause a nose-down pitching moment which through the effects of inertia coupling generally was such as to cause larger angles of sideslip and otherwise more violent maneuvers than would have existed without  $C_{m\beta}$ . For the X-3 airplane it appears that alinement of the principal axes with the flight path prior to rolling probably will lead to the least violent motions in roll. Increasing the directional stability also would cause a reduction in the violence of sideslip motions.

The results further indicate that the analysis of Phillips (NACA TN 1627) should be used primarily as a qualitative indication of the possible existence of divergent motions in rapid rolls. The initial conditions of the motion appear to be nearly as critical to the magnitude of motions encountered as does the proximity to the divergent boundary. It appears, at present at least, that extensive calculations using at least five degrees of freedom will be required to evaluate properly any given configuration.

~~CONFIDENTIAL~~

## INTRODUCTION

Recent flight experiences by the National Advisory Committee for Aeronautics on both the Douglas X-3 airplane and other types of fighter airplanes have indicated that extremely violent inadvertent coupled lateral and longitudinal motions can occur for such airplanes in rapid aileron rolls. (See refs. 1 and 2.) These motions were characterized by the attainment of very large angles of attack and sideslip and large load factors. Some analyses of these motions and explanations of their cause are presented in references 3 to 5. A fundamental theoretical analysis of this type of motion assuming constant rolling velocity was first made in references 6 and 7.

The investigations of references 2 and 3 were primarily of the motions of a swept-wing fighter airplane. A brief investigation also was made of the Douglas X-3 motions and the results of this study are presented herein.

## SYMBOLS

The forces, moments, and motions are referred to the body system of axes, which is shown in figure 1.

$C_L$  lift coefficient,  $\frac{L}{\frac{1}{2}\rho V^2 S}$

$C_Y$  lateral-force coefficient,  $\frac{Y}{\frac{1}{2}\rho V^2 S}$

$C_l$  rolling-moment coefficient,  $\frac{L'}{\frac{1}{2}\rho V^2 S b}$

$C_m$  pitching-moment coefficient,  $\frac{M}{\frac{1}{2}\rho V^2 S \bar{c}}$

$C_n$  yawing-moment coefficient,  $\frac{N}{\frac{1}{2}\rho V^2 S b}$

$C_D$	drag coefficient, $\frac{D}{\frac{1}{2}\rho V^2 S}$
$C_{N_A}$	airplane normal-force coefficient, $\frac{WA_z}{\frac{1}{2}\rho V^2 S}$
$C_{l_{\delta_a}}$	rate of change of rolling-moment coefficient with aileron deflection, per deg
$C_{n_{\delta_a}}$	rate of change of yawing-moment coefficient with aileron deflection, per deg
$C_{m_{i_t}}$	rate of change of pitching-moment coefficient caused by horizontal-tail deflection, per deg
$\delta_{a_t}$	aileron deflection, deg
$i_t$	horizontal-tail deflection, deg
$\delta_r$	rudder deflection, deg
$F_a$	aileron stick force, lb
$F_s$	elevator stick force, lb
$F_v$	rudder pedal force, lb
$L$	lift, lb
$D$	drag, lb
$Y$	lateral force, lb
$L'$	rolling moment, ft-lb
$M$	pitching moment, ft-lb
$N$	yawing moment, ft-lb
$S$	wing area, sq ft
$b$	wing span, ft
$\bar{c}$	mean aerodynamic chord, ft

$\rho$	air density, slugs/cu ft
$V$	velocity, ft/sec
$M'$	Mach number
$I_{X_0}, I_{Y_0}, I_{Z_0}$	moments of inertia about X, Y, and Z principal axes, respectively, slug-ft <sup>2</sup>
$I_X, I_Y, I_Z$	moments of inertia about X, Y, and Z body axes, respectively, slug-ft <sup>2</sup>
$K_X, K_Y, K_Z$	radii of gyration, nondimensionalized with respect to $b$
$I_{XZ}$	product of inertia (positive when principal axis is inclined below X body axis), slug-ft <sup>2</sup>
$I_{X_e}$	moment of inertia of rotating engine parts about X body axis, slug-ft <sup>2</sup>
$\mu_b$	relative density coefficient based on span, $m/\rho S b$
$\mu_c$	relative density coefficient based on chord, $m/\rho S \bar{c}$
$m$	mass of airplane, $W/g$ , slugs
$W$	weight of airplane, lb
$g$	acceleration due to gravity, 32.2 ft/sec <sup>2</sup>
$A_z$	normal acceleration divided by acceleration due to gravity
$A_y$	transverse acceleration divided by acceleration due to gravity
$\alpha$	angle of attack, $\tan^{-1} \frac{w}{u}$ , radians except when otherwise noted
$\Delta\alpha$	incremental angle of attack, deg
$\beta$	angle of sideslip, $\sin^{-1} \frac{v}{V}$ , radians except when otherwise noted
$u, v, w$	components of velocity $V$ along the X, Y, and Z body axes, respectively, ft/sec
$p$	rolling angular velocity, radians/sec
$q$	pitching angular velocity, radians/sec

- $r$  yawing angular velocity, radians/sec  
 $\omega_e$  engine rotational velocity, radians/sec  
 $\psi$  angle of yaw, radians  
 $\phi$  angle of roll, radians  
 $l, m, n$  direction cosines of X, Y and Z body axes from vertical, respectively  
 $t$  time, sec

$$C_{L_\alpha} = \frac{\partial C_L}{\partial \alpha}$$

$$C_{m_\alpha} = \frac{\partial C_m}{\partial \alpha}$$

$$C_{m_q} = \frac{\partial C_m}{\partial \frac{q \bar{c}}{2V}}$$

$$C_{m_\beta} = \frac{\partial C_m}{\partial \beta}$$

$$C_{l_\beta} = \frac{\partial C_l}{\partial \beta}$$

$$C_{n_\beta} = \frac{\partial C_n}{\partial \beta}$$

$$C_{Y_\beta} = \frac{\partial C_Y}{\partial \beta}$$

$$C_{l_p} = \frac{\partial C_l}{\partial \frac{p b}{2V}}$$

$$C_{n_p} = \frac{\partial C_n}{\partial \frac{p b}{2V}}$$

$$C_{l_r} = \frac{\partial C_l}{\partial \frac{rb}{2V}}$$

$$C_{n_r} = \frac{\partial C_n}{\partial \frac{rb}{2V}}$$

A dot over a symbol represents a derivative with respect to time.

Subscript o means initial condition.

#### METHOD OF ANALYSIS

The motion analysis was made by the solution of the equations of motion for five degrees of freedom, accomplished by the use of an electronic analog computer. The following equations of motion used herein were relative to the body axis:

$$\dot{p} = \left( \frac{I_Y - I_Z}{I_X} \right) qr + \frac{I_{XZ}}{I_X} (\dot{r} + pq) + \frac{\rho V^2 S b}{2 I_X} \left[ \left( C_{l_\beta} + \frac{\partial C_{l_\beta}}{\partial \alpha} \right) \beta + C_{l_{\delta_a}} \delta_{a_t} \right] + \frac{\rho V S b^2}{4 I_X} (C_{l_p} p + C_{l_r} r) \quad (1)$$

$$\dot{q} = \left( \frac{I_Z - I_X}{I_Y} \right) pr + \frac{I_{XZ}}{I_Y} (r^2 - p^2) - \frac{I_{X_e} \omega_e}{I_Y} r + \frac{\rho V^2 S \bar{c}}{2 I_Y} (C_{m_\alpha} \alpha + C_{m_\beta} \beta + C_{m_{i_t}} i_t) + \frac{\rho V S \bar{c}^2}{4 I_Y} C_{m_q} q \quad (2)$$

$$\dot{r} = \left( \frac{I_X - I_Y}{I_Z} \right) pq + \frac{I_{XZ}}{I_Z} (\dot{p} - qr) + \frac{I_{X_e} \omega_e}{I_Z} q + \frac{\rho V^2 S b}{2 I_Z} (C_{n_\beta} \beta + C_{n_{\delta_a}} \delta_{a_t}) + \frac{\rho V S b^2}{4 I_Z} (C_{n_r} r + C_{n_p} p) \quad (3)$$

$$\dot{\beta} = \frac{g_m}{V} - r + \alpha p + \frac{\rho VS}{2m} C_{Y\beta} \beta \quad (4)$$

$$\dot{\alpha} = \frac{g_n}{V} + q - \beta p - \frac{\rho VS}{2m} C_{L\alpha} \alpha - \frac{\rho VS}{2m} C_{D\alpha} \alpha \quad (5)$$

$$\left. \begin{aligned} \dot{i} &= mr - nq \\ \dot{m} &= np - lr \\ \dot{n} &= lq - mp \end{aligned} \right\} \quad (6)$$

The linear velocity  $u$  along the X body axis was assumed to be constant and the sixth equation of motion was neglected. Because of the limited computer equipment available, equations (4) and (5) (as shown) were used in a simplified form. This simplification consisted of assuming that  $\sin \alpha$  and  $\sin \beta$  were approximately equal to  $\alpha$  and  $\beta$ , respectively, that  $\cos \alpha$  and  $\cos \beta$  were approximately equal to one, and that the resultant velocity  $V$  was constant. It should be mentioned that in other unpublished studies comparison between a complete motion calculation involving six degrees of freedom and a motion involving five degrees of freedom as used herein has shown very good agreement; thus the use of the five-degrees-of-freedom solution and the previously mentioned simplifications is justified. Equations (6) were used to determine the direction cosine of the body axis from the vertical.

#### CALCULATIONS

The most violent motion of the Douglas X-3 airplane occurred at a Mach number of about 1.05 at 30,000 feet (ref. 1); accordingly, the calculations were made to evaluate this particular maneuver. Figure 2 (taken from ref. 1) is a flight record of this maneuver. Unfortunately, aerodynamic data were most scarce at this speed. The results of reference 8, which presents derivatives obtained on a rocket model of the configuration, were for angles of attack near zero and were used in part for determining the actual derivatives for the calculations. References 9, 10, and 11 were also used in determining the values used. A table of values of the aerodynamic characteristics used for the basic calculations is shown in table I. Also listed in table I are the geometric, mass, and inertia characteristics of the airplane.



~~CONFIDENTIAL~~

The derivatives are given relative to the body axis as used in the calculation. The inertia characteristics, including the inclination of the principal axis, were based on estimates used for studies of a similar configuration in references 12 and 13. Preliminary calculations indicated that values of  $C_{l_\beta}$  as large as those indicated by existing wind-tunnel and rocket-model data would not allow for the calculation of a motion nearly representing that obtained by the airplane. Accordingly, the values of  $C_{l_\beta}$  as shown in figure 3 were adjusted for better correlation and were considerably smaller than those indicated by test data. The results of wind-tunnel tests (refs. 9 and 14) at both supersonic and low subsonic speeds show that the vertical tail is a major contributor to a stable  $C_{l_\beta}$  for this airplane. Negative and neutral dihedral effectiveness, respectively, exist at these speeds with the vertical tail off. Thus, flexibility of the vertical tail and the rear fuselage, and jet effects on the vertical tail could justify some reduction in  $C_{l_\beta}$  as well as the use of a somewhat smaller value of  $C_{n_\beta}$  than was indicated by reference 9.

The value of the angle of attack at the beginning of the rolling motion, as indicated by the airplane flight record, was about  $3.4^\circ$ . (See fig. 2.) Based on available experimental data (refs. 9, 10, and 11) of the angle of attack for zero lift and the lift-curve slope, the angle of attack of  $3.4^\circ$  (for the lift necessary to give 0.65g (fig. 2) at the beginning of the flight and for the value of  $i_t$  of  $-1.6^\circ$  used at the beginning of the motion) appears to be too large. Accordingly, several initial angles of attack ( $1.8^\circ$ ,  $2.4^\circ$ ,  $3.4^\circ$ , and  $4.4^\circ$ ) were studied. From the available information on the angle of attack for zero lift and for the lift-curve slopes of references 9 and 10 and that measured approximately from flight (ref. 11), the actual angle of attack for the flight was probably between  $2.5^\circ$  and  $3.0^\circ$ .

Values of changes in pitching moment with sideslip also were simulated in the calculations. The data of  $C_m$  plotted against  $\beta$  that were available and the value of  $C_{m_\beta}$  used in the calculations are shown in figure 4. Because of equipment limitations,  $C_{m_\beta}$  was simulated as a constant on the analog, and the sign was changed with the sign of  $\beta$  so as always to give a negative increment in  $C_m$ . Because the available data (ref. 9) show an increasing value of  $C_m$  with  $\beta$  at the largest value of  $\beta$  for which data are available ( $6^\circ$ ), some calculations were made with a larger value of  $C_{m_\beta}$  than indicated in figure 4.

Results of reference 9 indicate that between the Mach numbers of 1.05 and 0.95 an angle-of-attack trim change exists. This trim change is in

the nose-down sense when the speed is decreasing and a simulation of this was made for a few calculations by introducing an equivalent step change in pitching moment which was maintained in the calculation for the complete motion. The effects of changes in  $C_{n\beta}$  and in the direction of roll on the motions in rolls were also investigated.

The control manipulations used for the actual flight are shown in figure 2, along with the rest of the flight record. For the calculations, which simulate only about the first five seconds of the motion, the rudder was held fixed at neutral ( $\delta_r = 0$ ), the stabilizer  $i_t$  was moved exactly as it was in flight by the use of an input-output table, and the aileron input  $\delta_{a_t}$  was represented by a trapezoidal type of impulse most nearly simulating the actual input.

Knowledge obtained subsequent to the time of the calculations contained herein indicates that the motion from reference 1 (fig. 2) was made at a pressure altitude of 24,700 feet rather than 30,000, and that the moments of inertia  $I_Y$  and  $I_Z$  used in this paper might be as much 20 percent low. Because of these factors (although they tend to be compensating) and other factors associated with the aerodynamic characteristics and trim angles of attack previously discussed, the results herein are primarily of qualitative value. Although the correlation between flight and calculation will be shown to be fair, the actual quantitative values of course may not be considered to be any more accurate than the characteristics used in the calculations.

## RESULTS AND DISCUSSION

In order to obtain a reasonable correlation between the flight motion measured on the airplane and the calculations, certain adjustments were made, as noted under "Calculations." Figure 5 shows a comparison of the flight results with calculations for five degrees of freedom with an initial angle of attack of  $1.8^\circ$ . The five-degrees-of-freedom calculation, although not precisely duplicating the actual flight motion, does show large variations in the components of the motion of the order of magnitude of the actual flight record. This five-degrees-of-freedom calculation was thus assumed to be a basis for comparison in evaluating the effects of some parameters on the motion.

A significant factor in this motion, both in flight and in the calculations, is that the most violent phase of the motion occurs after the aileron has been taken off to stop the roll. The rolling velocity reduced and approached zero at the time when the greatest magnitudes in the other components of motion tended to exist. The significance of this is that as

the motion progressed certain components of the motion, particularly in equations (4) and (5) for  $\dot{\alpha}$  and  $\dot{\beta}$ , developed in a manner to compensate one another. Thus, when the rolling velocity was reduced,  $\dot{\alpha}$  was influenced by a relatively large pitching velocity which had been tending to balance the  $\beta p$  component (eq. (5)) and  $\dot{\beta}$  was influenced by a relatively large yawing velocity which in part had been balanced by the  $\alpha p$  component (eq. (4)). The maximum values of  $\alpha$  and  $\beta$  occurred at times when  $q$  and  $r$  changed signs, respectively, and after  $p$  was appreciably reduced. This effect has occurred on almost all the dangerous maneuvers which have been encountered in flight (see refs. 1 and 2); therefore, consideration of the recovery phase of a rolling motion, particularly one which has penetrated a roll divergence boundary (ref. 6), seems essential in the study of any design.

In conjunction with this discussion, the stabilizer  $i_t$  was moved up at the time the angle of attack was in a negative sense and the pitching velocity was greatest negatively. (See fig. 2.) The rapid change in angle of attack which occurred when the pitching velocity changed sign was augmented by this stabilizer movement causing an even more violent change in angle of attack and normal acceleration than would have occurred otherwise. The stabilizer control movement which was logical from the sense of accelerations felt by the pilot was thus actually detrimental to the motion. Such a significant effect has been noted by other investigators. (See, for example, ref. 15.)

#### Effect of Principal-Axis Inclination

The effects of principal-axis inclination to the flight path were studied by adjusting the angle of attack for zero lift. Angles of attack ranging from  $1.8^\circ$  to  $4.4^\circ$  were studied, as has been noted previously. The results of this study are shown in figure 6. The principal axis was inclined  $3.5^\circ$  (based on estimations) below the X body axis. Thus, at  $1.8^\circ$  angle of attack the principal axis was inclined  $1.7^\circ$  below the flight path. This inclination of the axis caused the generation of the right sideslip in a left roll. In general, in a rolling motion this situation is essential to the development of sideslip of sign opposite to the sign of the rolling velocity, particularly when the yawing moments due to aileron deflection and rolling are adverse. Large positive values of  $C_{n_p}$  (several times larger than those used) or a large favorable yawing moment from the ailerons (larger and opposite in sign to that used here), however, might also cause positive sideslip to occur in left rolls.

If the equations of motion relative to the principal axis are considered,  $\dot{r}$  and  $r$  would be negligible at the beginning of the motion as  $I_{YZ}$  is zero and provided  $C_{n_p}$  and  $C_{n_{\delta_a}} \delta_a$  were small; thus, in equation (4) the only term to generate sideslip is  $\alpha p$ . Positive sideslip in

a left (negative) roll can thus only be generated if  $\alpha$  of the principal axis has a negative value.

Further, if the equations of motion relative to a system of axis alined initially with the wind are considered, the angle of attack is zero and  $\dot{\beta}$  (eq. (4)) can only be affected by  $r$ . The yawing velocity  $r$  through  $\dot{r}$  depends initially on the product of inertia term  $\frac{I_{XZ}\dot{p}}{I_Z}$  (provided, as before,  $C_{n_p}$  and  $C_{n_{\delta_a}}$  were small) so that the sign of  $\dot{\beta}$  through  $\dot{\beta}$  is dependent on the sign of  $I_{XZ}$ , which is positive if the principal axis is below or negative if the principal axis is above the axis system alined with the wind or flight path; thus, in another manner it is seen that the principal axis must be below the flight path to attain sideslip angles opposite in sign to the rolling velocity.

From the standpoint of the equations of motion about the body axis, this motion occurs from the existence of a negative  $\dot{r}$  occurring immediately in the motion from  $\frac{I_{XZ}\dot{p}}{I_Z}$  (eq. (3)) which in turn gives a negative  $r$  in the  $\dot{\beta}$  equation (eq. (4)). In equation (4) the negative value of  $r$  is opposed by the  $\alpha_p$  term,  $\alpha$  now being the angle of attack of the body axis. Depending on the relative magnitudes of  $\alpha_p$  and  $r$  in equation (4), the sideslip angle can be either positive or negative. The attainment of positive sideslip in a left roll depends, then, on  $r$  being larger than  $\alpha_p$ ; this situation occurs when the initial angle of attack is small, as is the case for the present paper. From this discussion it appears that, except for yawing moments occurring from rolling  $C_{n_p}$  and from the ailerons  $C_{n_{\delta_a}}$  or from other extraneous inputs, no motion but that of rolling can occur when the principal axis is alined with the flight path.

In figure 6 the results show that, as the angle of attack is increased to  $3.4^\circ$  (principal axis about on the flight path), the motion in sideslip is small (about  $2^\circ$  maximum) and, as the angle of attack is increased to  $4.4^\circ$ , the initial sideslip angle is of the same sign as the rolling velocity. The other components of the motion, in general, decrease in violence, as does the sideslip angle, when the inclination of the principal axis is changed. The rolling velocity changes somewhat with principal-axis inclination from the effects of the rolling moment due to sideslip.

Study of the steady rolling characteristics of this airplane on the basis of the linearized analysis of reference 6 is indicated in figure 7. Because the directional stability varied with angle of attack, the directional stabilities based on the initial angle of attack were

used to construct figure 7. For all the angles of attack, the rolling velocity exceeded that which is estimated as critical from the intersections of the boundaries of figure 7. The motions, however, are greatly different and those at angles of attack of  $3.4^\circ$  and  $4.4^\circ$  - at least appear not to have a dangerous divergence character that exists for the motion at  $1.8^\circ$ . (See fig. 6.) Based on previous discussions, the primary difference in these motions is the input to the motion, where the input is derived from the initial angle of attack. Thus, it is indicated that the initial conditions of the motion are as critical to the type or dangerous character of the motion as is the penetration of a critical or unstable rolling-velocity regime. It is realized, of course, that once a critical rolling velocity is exceeded extraneous inputs could cause a dangerous divergence even for the relatively mild motion occurring when  $\alpha_0 = 3.4^\circ$ . The degree of penetration beyond the divergence boundary and the time spent at or above critical rolling velocities could also influence the dangerous aspects of the motion and for the cases calculated might have had some influence. It is important to note, however, that the motion at  $\alpha_0 = 4.4^\circ$ , which penetrates least and for the least time (for the cases calculated) has a greater magnitude of motion than does the motion at  $\alpha_0 = 3.4^\circ$ ; this fact reemphasizes the significance of the initial conditions or inputs to the motion.

The significance of these observations is that, although reference 6 gives an indication of the potential danger of rolling divergences, extreme care must be exercised in its application to rapid transient rolling problems. It appears, then, that more precise motion calculations are needed in each specific case; with particular regard being given to the initial and input conditions in order to properly evaluate the degree of difficulty that may be encountered.

#### Effect of Changes in Directional Stability

The results of references 3, 4, and 6 indicate the possibility of improving the rolling divergence problem by increasing the directional stability. The calculated effects of changing the directional stability are shown in figure 8. When the stability was cut in half, the motion was greater in its maximum magnitude than was the basic motion, and the sideslip angle exceeded the recording limits of the analog computer. Up to a time of about  $3\frac{1}{2}$  seconds, the motion with reduced directional stability was not significantly different from the basic case. Subsequent to this time, however, the sideslip increases rapidly and thus causes the rolling velocity to increase in magnitude through dihedral effectiveness despite the aileron deflection. The somewhat larger negative yawing velocities due to reduced stability which, in turn, tended to cause less negative pitching velocities appear to have been primary causes for this general effect.

Increasing the stability to one and one-half and to two times the basic value gave very substantial improvements in magnitude of sideslip encountered, although up to about 3 seconds no significant difference in sideslip appeared; whereas the angle of attack and angular velocities were generally lower in magnitude than for the basic case up to this time. The reduced pitching and yawing velocities were, of course, the basis for improvement in that they approached zero progressively earlier in the motion (after aileron movement to stop the roll) as the stability increased and thus caused the maximum angles of attack and sideslip also to occur earlier. Near the end of the motion, slightly more violent variations in angle of attack and pitching velocity appear to have occurred for the increased-stability cases than for the basic case. The stabilizer movement (previously discussed) had a different influence on these cases near the end of the motion because the timing of the rearward stick movement was effectively different; the logical manipulation of the stabilizer (from the pilot's sense) for the flight case may have been less logical for the increased stability cases than for the original case because of these timing effects.

A study of the effects of changes in  $C_{n\beta}$  on the steady rolling characteristics on the basis of the linearized analysis of reference 6 is indicated in figure 9. The indications from this figure are that for the larger directional stabilities ( $C_{n\beta} = 0.33$  and  $C_{n\beta} = 0.44$ ) regimes of divergence in steady rolling are avoided. From figure 8 angles of sideslip of the order of  $12^\circ$  and  $8^\circ$ , respectively, were obtained for these conditions of increased stability; these motions are fairly large although presumably stable. The initial conditions of the motion undoubtedly influence these magnitudes for, as previously discussed, when the initial angle of attack was  $3.4^\circ$  or  $4.4^\circ$  (figs. 6 and 7), smaller magnitudes of motion were obtained than were obtained with increased stability (figs. 8 and 9), despite the fact that the motions of figures 6 and 7 were presumably unstable.

#### Effect of Pitching Moment Due to Sideslip

As has been noted previously, the pitching moment due to sideslip was simulated in the calculations. In order to determine the influence of this derivative on the airplane motion,  $C_{m\beta}$  was set to zero. The result of a comparison with the basic motion is shown in figure 10(a). The angle of sideslip was reduced from approximately  $20^\circ$  maximum for the basic case to  $8^\circ$  when  $C_{m\beta}$  was zero. The angle-of-attack variations were also less violent than for the basic motion. Thus, there exists a very important influence of a heretofore neglected aerodynamic derivative. The aerodynamic causes for the existence of pitching moment due to

sideslip and the influences of various geometric parameters on this derivative are discussed in reference 16. As noted in reference 16,  $C_{m\beta}$  can cause pitching moments of either a positive or negative sense, and thus pitching moments due to sideslip will not always have a detrimental effect as for the present case.

The influence of increasing  $C_{m\beta}$  on motions wherein the directional stability  $C_{n\beta}$  has been increased are included in figure 10(b). These results show further the rather important effect of  $C_{m\beta}$  even for cases outside regimes of steady rolling divergence. For the case where  $C_{n\beta} = 0.33$ , increasing  $C_{m\beta}$  by about fifty percent increased the violence of the calculated motion considerably;  $\beta$  increased from  $12^\circ$  to something over  $20^\circ$ . With  $C_{n\beta} = 0.44$  a similar increase in  $C_{m\beta}$  caused an increase in maximum  $\beta$  of from  $8^\circ$  to  $12^\circ$  and influenced the rest of the motion considerably. As noted previously, the values of  $C_{m\beta}$  used may have been optimistically small for the large angles of sideslip attained because of its nonlinear character, and values larger than those used may have existed in flight and could have accounted for relatively larger motion attained in flight than in the calculations at angles of attack between  $2.4^\circ$  and  $3.4^\circ$ , where the flight probably was initiated. It is significant to realize that pitching moments from any source (sideslip, control inputs, etc.) can have a major influence on the motion, although such moments have no influence on the rolling velocity predicted for divergence by reference 6. The importance of analog computations to evaluate properly the dangerous or violent aspects of a motion whether unstable or not is thus emphasized by these results.

#### Effects of Trim Changes

Another significant effect was found from the introduction of a trim change due to Mach number (as may occur near Mach number 1 where the Douglas X-3 flight maneuver was performed. (See ref. 8)). The out-of-trim moment used to represent this trim change was introduced to the problem (as previously noted) by adding an incremental stabilizer deflection at zero time which gave an equivalent out-of-trim moment equal to that due to an angle of attack of  $1^\circ$ . The effect of the addition of this trim change moment is shown on figure 11. This effect is compared with the basic case minus the influence of  $C_{m\beta}$ . Here again an appreciable increase in  $\beta$  and the other components of motion is evident.

The influence during rapid rolls of such an inherent factor as this trim change due to Mach number (similar to the case of  $C_{m\beta}$ ) would not

affect the divergence boundaries predicted by reference 6. This rather significant influence of inherent pitching moments in rolling motions, similar to that of the effects of principal-axis inclination (previously discussed) must be studied therefore by calculations similar to those presented herein.

The effects discussed for out-of-trim moments and even pitching moments due to sideslip are also representative of the effects that would occur because of inadvertent stick movements. The cases presented herein effectively represent forward stick motions (nose-down pitching moments) which for this particular configuration and flight condition are detrimental. The implication of these results is that nose-up pitching moments or rearward stick movements would be beneficial for this case. This cannot be a general conclusion, in that for other configurations and even for other flight conditions for the present configuration the reverse situation could be true. The sense of the effectiveness of applied pitching moments during rolling maneuvers may be inherently associated with the existence of sideslip angles of the same or opposite sign as the rolling velocity occurring as the roll progresses because of the coupling effects due to pitching velocity. The timing of such control applications is evidently very critical, however, for nose-up pitching moments, which have been implied to be beneficial during the roll, were detrimental to the motion when applied during the recovery from the roll, as was previously discussed.

#### Effect of Roll Direction

Experience on the Douglas X-3 airplane has indicated that the motions resulting from left and right rolls were considerably different. A study was made, therefore, of the effect of roll direction. The results are presented in figure 12 for the various angles of attack from  $1.8^\circ$  to  $4.4^\circ$  that were previously discussed and were shown in figure 6. The basic motion has been for a left roll with the engines running conventionally (clockwise from the rear). For the comparative right rolls in figure 12, the values of  $\beta$ ,  $p$ , and  $r$  for ease of comparison have been plotted with opposite signs so as to have the same signs as do these components of motion in left rolls. The results, in general, show a more violent motion in the right rolls, particularly when the angle of attack of the principal axis was negative.

The differences in left and right rolls, of course, derive directly from two terms in the equations of motion -  $\frac{I_{Xe} \omega_e}{I_Z} q$  in the yawing-moment equation (eq. (3)) and  $\frac{I_{Xe} \omega_e}{I_Y} r$  in the pitching-moment equation (eq. (2)). The first of these terms gives a negative yawing acceleration for both



right and left rolls because of the negative pitching velocities acting for this investigation, which, in turn, would cause a positive increment of sideslip angle to exist for both directions of roll. For the motions in figure 12, where the sideslip is positive (left rolls), this then is detrimental whereas it is favorable for the right rolls. This conclusion is contrary, however, to the results of figure 12; the indication is

that the dominant effect of engine rotation must have come from  $\frac{I_x \omega_e}{I_y} r$ .

This moment is nose-up in the left rolls and nose-down in the right rolls, and thus a larger negative pitching velocity in the right rolls than the left is caused. This larger negative pitching velocity acting

through the pitch-roll cross-coupling term  $\frac{I_x - I_y}{I_z} p q$  in the yawing-

moment equation (eq. 3) caused larger values of positive yawing velocity in right rolls than negative yawing velocity in left rolls, in spite of the other engine-momentum term previously discussed. The larger yawing velocity in right rolls than in left rolls led to larger magnitudes of sideslip in the right rolls. The total effect of roll direction is not completely explained by the above discussion because of the compounding effects that occur from other factors such as  $C_{m\beta}$ , for example. The basic effect of roll direction is initiated, however, in the manner discussed.

In that the major effect of roll direction appears to have come from the pitching moment acting, all previous discussions relating to the pitching moments are applicable in a general sense to the effects of engine momentum. Of significance is the fact that the right rolls are more violent than left rolls (fig. 12) except for the case where the principal axis is above the flight path ( $\alpha = 4.4^\circ$ ) or, more appropriately, when the sideslip is of the same sign as the rolling velocity. Thus, the increment in nose-down pitching velocity from the engine momentum in right rolls is detrimental when the sideslip is of the opposite sense of the rolling velocity and favorable when the sideslip is of the same sense as the rolling velocity. This latter case is the same as that treated in reference 17 where left rolls were shown to have somewhat lower critical rolling velocities than right rolls.

#### SUMMARY OF RESULTS

The results of an analytical investigation of rapid rolling motions of the Douglas X-3 airplane and comparisons with flight experience indicate that the violent lateral-longitudinal coupling motions encountered on the X-3 were apparently caused by the inclination of the principal axis below the flight path at the onset of the rolling maneuvers and the

existence of a value of pitching moment due to sideslip  $C_{m\beta}$ , possibly combined with a trim change near Mach number 1. The inclination of the principal axis below the flight path caused the sideslip to be positive in left rolls which, in turn, created a rolling moment due to dihedral effectiveness  $C_{l\beta}$  which tended to increase the rolling velocity to critical values. The pitching moment due to sideslip  $C_{m\beta}$  was such as to cause a nose-down pitching moment which through the effects of inertia coupling generally was such as to cause larger angles of sideslip and otherwise more violent maneuvers than would have existed without  $C_{m\beta}$ . For the Douglas X-3 airplane it appears that starting rolls at somewhat larger angles of attack and possibly the use of airplane nose-up pitching moments at the very onset of a roll would tend to avoid the violent motions encountered. Alinement of the principal axis with the flight path prior to rolling probably will lead to the least violent motions in roll. Increasing the directional stability  $C_{n\beta}$  also would cause a reduction in the violence of motions.

The results further indicate that the analysis of Phillips (NACA TN 1627) should be used primarily as a qualitative indication of the possible existence of danger in rapid rolls. The initial conditions of the motion, such as the angles of attack and control inputs, particularly pitching moment inputs, appear to be nearly as critical to the magnitude of motions encountered as does the proximity to the steady-rolling divergent boundary. It appears, at present at least, that extensive calculations using at least five degrees of freedom will be required to evaluate properly any given configuration.

Langley Aeronautical Laboratory,  
National Advisory Committee for Aeronautics,  
Langley Field, Va., February 29, 1956.

## REFERENCES

1. NACA High-Speed Flight Station: Flight Experience With Two High-Speed Airplanes Having Violent Lateral-Longitudinal Coupling in Aileron Rolls. NACA RM H55A13, 1955.
2. Sisk, Thomas R., and Andrews, William H.: Flight Experience With a Delta-Wing Airplane Having Violent Lateral-Longitudinal Coupling in Aileron Rolls. NACA RM H55H03, 1955.
3. Gates, Ordway B., Jr., Weil, Joseph, and Woodling, C. H.: Effect of Automatic Stabilization on the Sideslip and Angle-of-attack Disturbances in Rolling Maneuvers. NACA RM L55E25b, 1955.
4. Weil, Joseph, Gates, Ordway B., Jr., Banner, Richard D., and Kuhl, Albert E.: Flight Experience of Inertia Coupling in Rolling Maneuvers. NACA RM H55E17b, 1955.
5. Zimmerman, Charles H.: Recent Stability and Aerodynamic Problems and Their Implications as to Load Estimation. NACA RM L55E11a, 1955.
6. Phillips, William H.: Effect of Steady Rolling on Longitudinal and Directional Stability. NACA TN 1627, 1948.
7. White, R. J., Uddenberg, R. C., Murray, D., and Graham, F. D.: The Dynamic Stability and Control Equations of a Pivoted-Wing Supersonic Pilotless Aircraft, With Downwash, Wake and Interference Effects Included. Doc. No. D-8510, Boeing Aircraft Co., Jan. 9, 1948.
8. Mitchell, Jesse L., and Peck, Robert F.: Investigation of the Lateral Stability Characteristics of the Douglas X-3 Configuration at Mach Numbers From 0.6 to 1.1 by Means of a Rocket-Propelled Model. NACA RM L54L20, 1955.
9. Olson, Robert N., and Chubb, Robert S.: Wind-Tunnel Tests of a 1/12-Scale Model of the X-3 Airplane at Subsonic and Supersonic Speeds. NACA RM A51F12, 1951.
10. Peck, Robert F., and Hollinger, James A.: A Rocket-Model Investigation of the Longitudinal Stability, Lift, and Drag Characteristics of the Douglas X-3 Configuration With Horizontal Tail of Aspect Ratio 4.33. NACA RM L53F19a, 1953.
11. Bellman, Donald R., and Murphy, Edward D.: Lift and Drag Characteristics of the Douglas X-3 Research Airplane Obtained During Demonstration Flights to a Mach Number of 1.20. NACA RM H54I17, 1954.

12. Stone, Ralph W., Jr.: Estimation of the Maximum Angle of Sideslip for Determination of Vertical-Tail Loads in Rolling Maneuvers. NACA Rep. 1136, 1953. (Supersedes NACA TN 2633.)
13. Stone, Ralph W., Jr.: An Analytical Study of Sideslip Angles and Vertical-Tail Loads in Rolling Pullouts As Affected by Some Characteristics of Modern High-Speed Airplane Configurations. NACA RM L53G21, 1953.
14. Delany, Noel K., and Hayter, Nora-Lee F.: Low-Speed Investigation of a 0.16-Scale Model of the X-3 Airplane - Lateral and Directional Characteristics. NACA RM A51A16, 1951.
15. Weil, Joseph, and Day, Richard E.: An Analog Study of the Relative Importance of Various Factors Affecting Roll Coupling. NACA RM H56A06, 1956.
16. Polhamus, Edward C.: Some Factors Affecting the Variation of Pitching Moment With Sideslip of Aircraft Configurations. NACA RM L55E20b, 1955.
17. Gates, Ordway B., Jr., and Woodling, C. H.: A Theoretical Analysis of the Effect of Engine Angular Momentum on Longitudinal and Directional Stability in Steady Rolling Maneuvers. NACA RM L55G05, 1955.

TABLE I

## DOUGLAS X-3 AIRPLANE CHARACTERISTICS USED IN CALCULATIONS

(a) Mass and dimensional characteristics and flight conditions		(b) Aerodynamic coefficients and derivatives	
		[All derivatives are with respect to radians except when otherwise noted]	
W, lb . . . . .	20,828	$C_{L,0}$ . . . . .	0.168
m, slugs . . . . .	647	$C_{L\alpha}$ . . . . .	5.33
S, sq ft . . . . .	166.5	$C_{m\alpha}$ . . . . .	-1.29
b, ft . . . . .	22.7	$C_{mq}$ . . . . .	-12.00
$\bar{c}$ , ft . . . . .	7.84	$C_{m\beta}$ , (nose down for	
$I_x$ , slug-ft <sup>2</sup> . . . . .	5,381	all values of $\beta$ ) . .	0.364
$I_y$ , slug-ft <sup>2</sup> . . . . .	63,971	$C_{m\dot{\alpha}}$ , per deg . . . . .	-0.045
$I_z$ , slug-ft <sup>2</sup> . . . . .	65,559	$C_{l_p}$ . . . . .	-0.40
$I_{xz}$ , slug-ft <sup>2</sup> . . . . .	3,700	$C_{l_r}$ . . . . .	0.20
V, ft/sec . . . . .	1046	$C_{l_\beta}$ . . . . .	-0.0175
$M'$ . . . . .	1.05	$\frac{\partial C_{l_\beta}}{\partial \alpha}$ . . . . .	-0.331
Altitude, ft . . . . .	30,000	$C_{n_p}$ . . . . .	0.10
$A_{z_0}$ , g units . . . . .	0.65	$C_{n_r}$ . . . . .	-1.50
$q_0$ , radians/sec . . . . .	-0.01081	$C_{n_\beta}$ . . . . .	0.22
$\frac{1}{2}\rho V^2$ , lb/sq ft . . . . .	485	$C_{Y_\beta}$ . . . . .	-0.91
$\frac{I_z - I_x}{I_y}$ . . . . .	0.941	$C_{l_{\delta_a}}$ , per deg . . . . .	0.00111
$\frac{I_y - I_z}{I_x}$ . . . . .	-0.295	$C_{n_{\delta_a}}$ , per deg . . . . .	-0.000195
$\frac{I_x - I_y}{I_z}$ . . . . .	-0.8935		
$I_{x_e} \omega_e$ , lb-ft-sec . . . . .	26,350		
Center-of-gravity location, percent $\bar{c}$ . . . . .	5		
Principal-axis inclination, deg . . . . .	3.5		

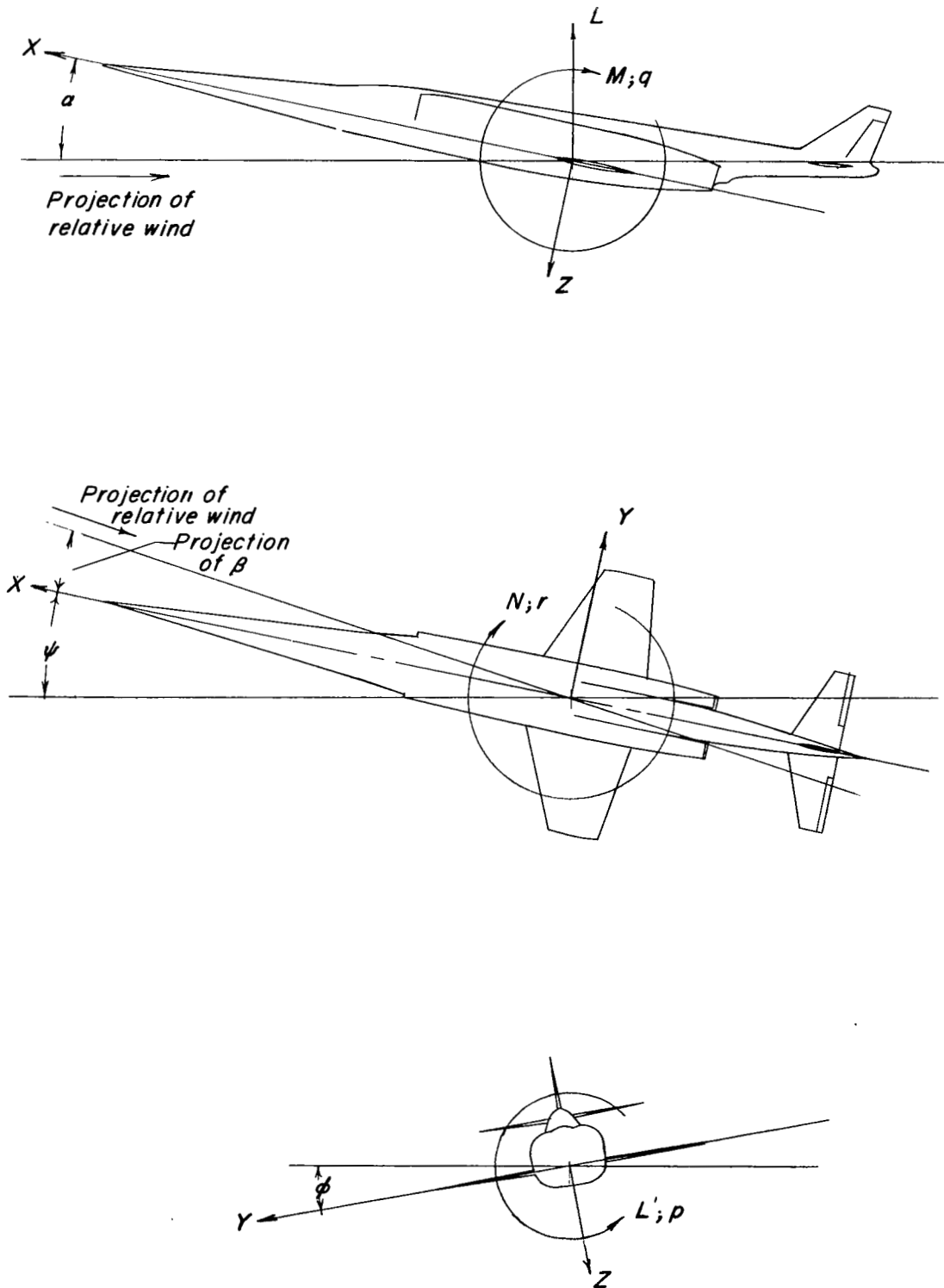


Figure 1.- Sketch depicting the body axis system. Each view presents a plane of the axis system as viewed along the third axis.

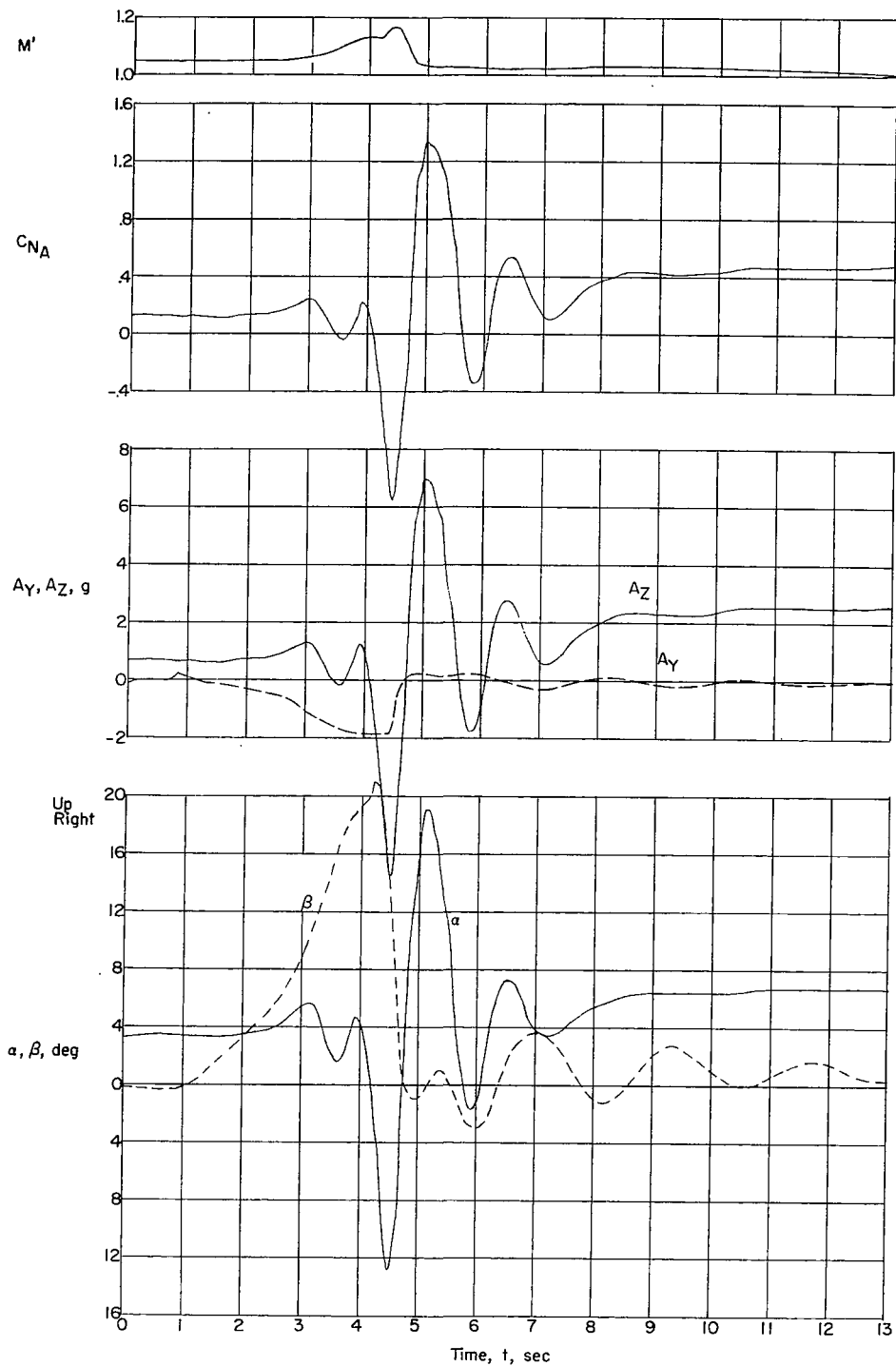


Figure 2.- Time histories of quantities measured during an abrupt aileron roll with the Douglas X-3 airplane at  $M' = 1.05$  and at a pressure altitude of 30,000 feet. (Data from ref. 1.)

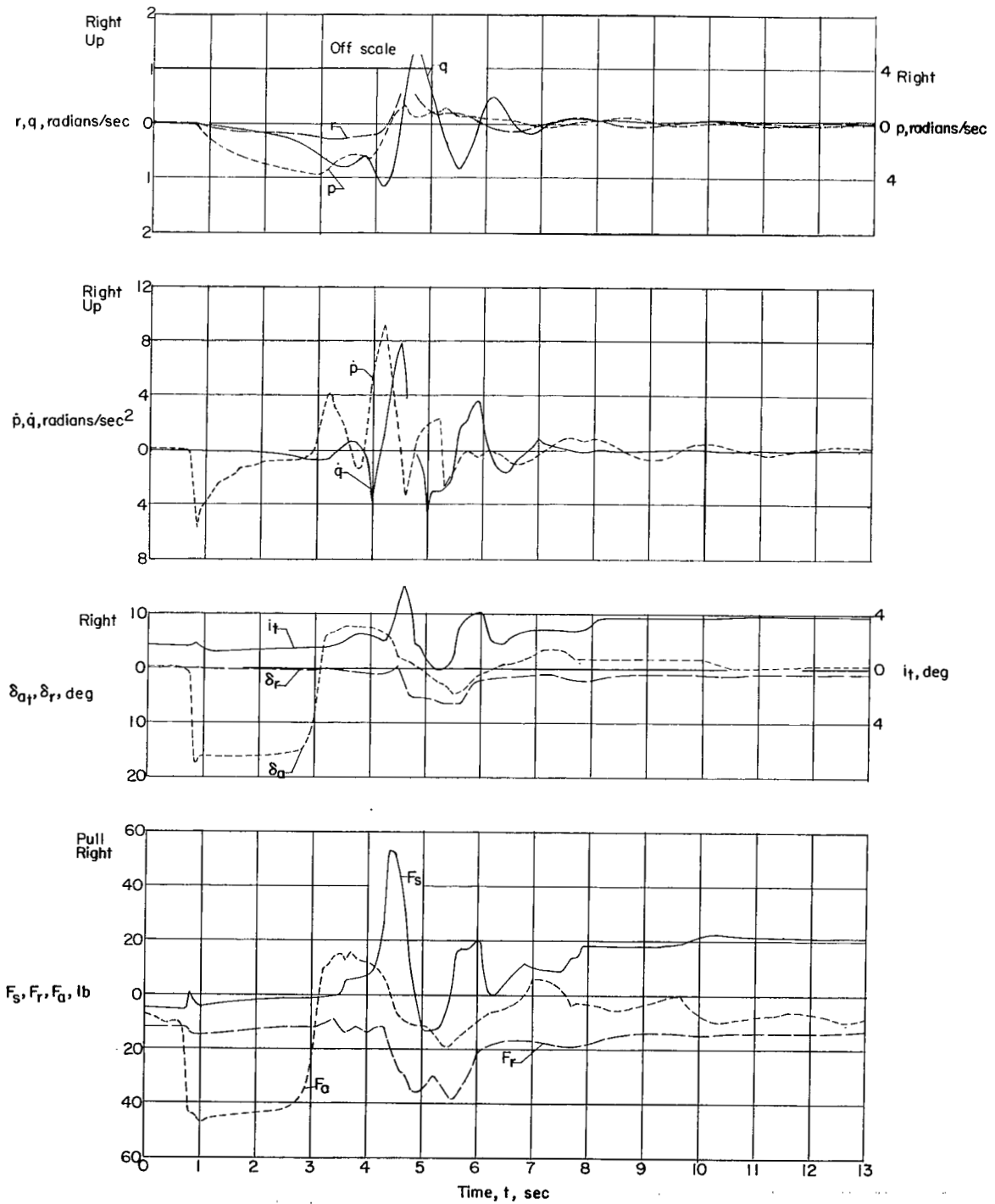


Figure 2.- Concluded.



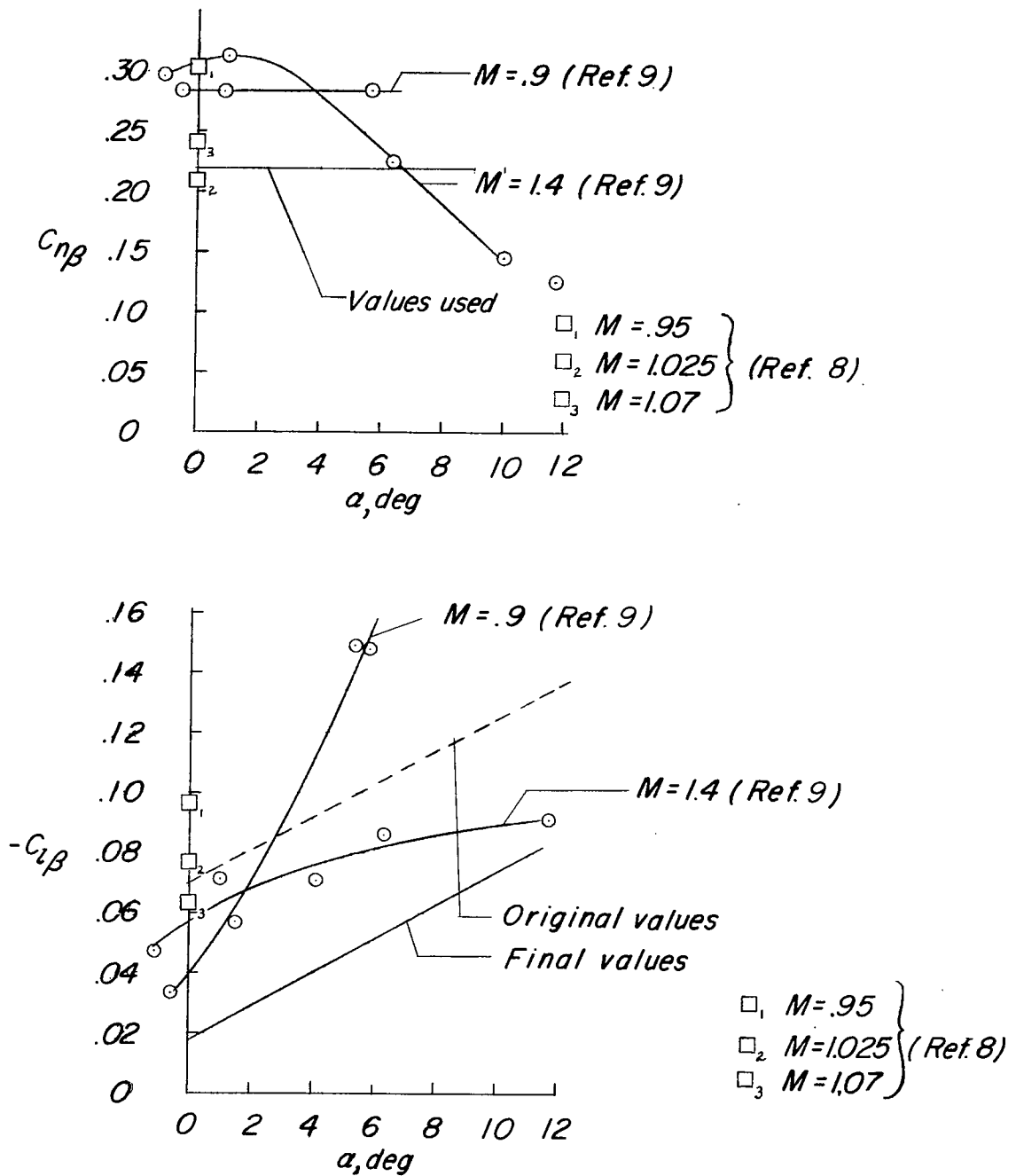


Figure 3.- Variations of the sideslip derivatives  $C_{n\beta}$  and  $C_{l\beta}$  with angle of attack from various sources and those used in the calculations.

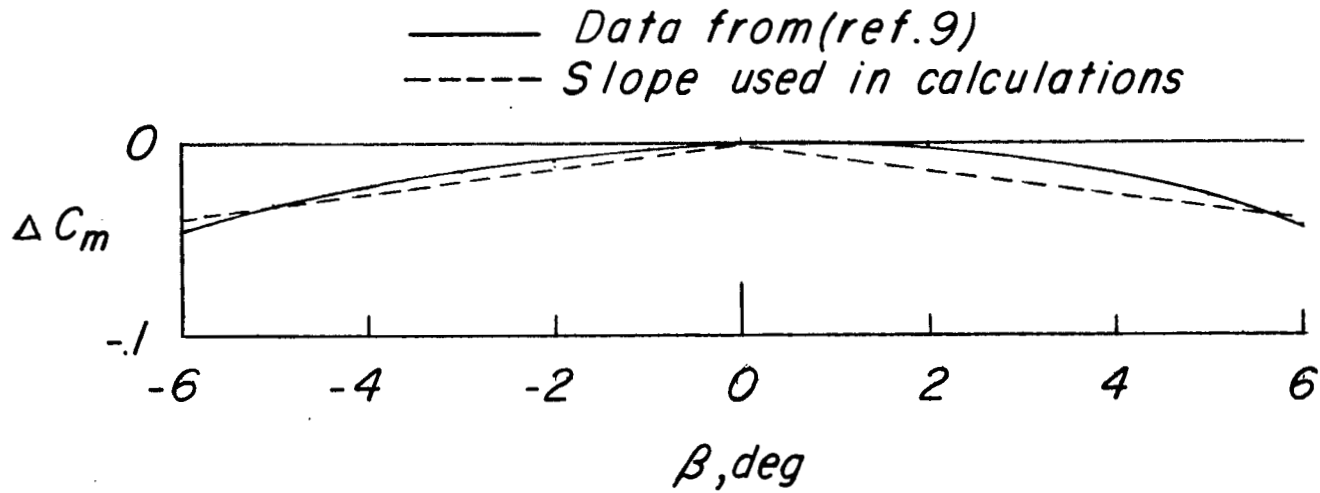


Figure 4.- A comparison of measured pitching moment with sideslip angle and values used for calculations. Slope  $C_{m\beta}$  used in calculations was independent of  $\alpha$ .

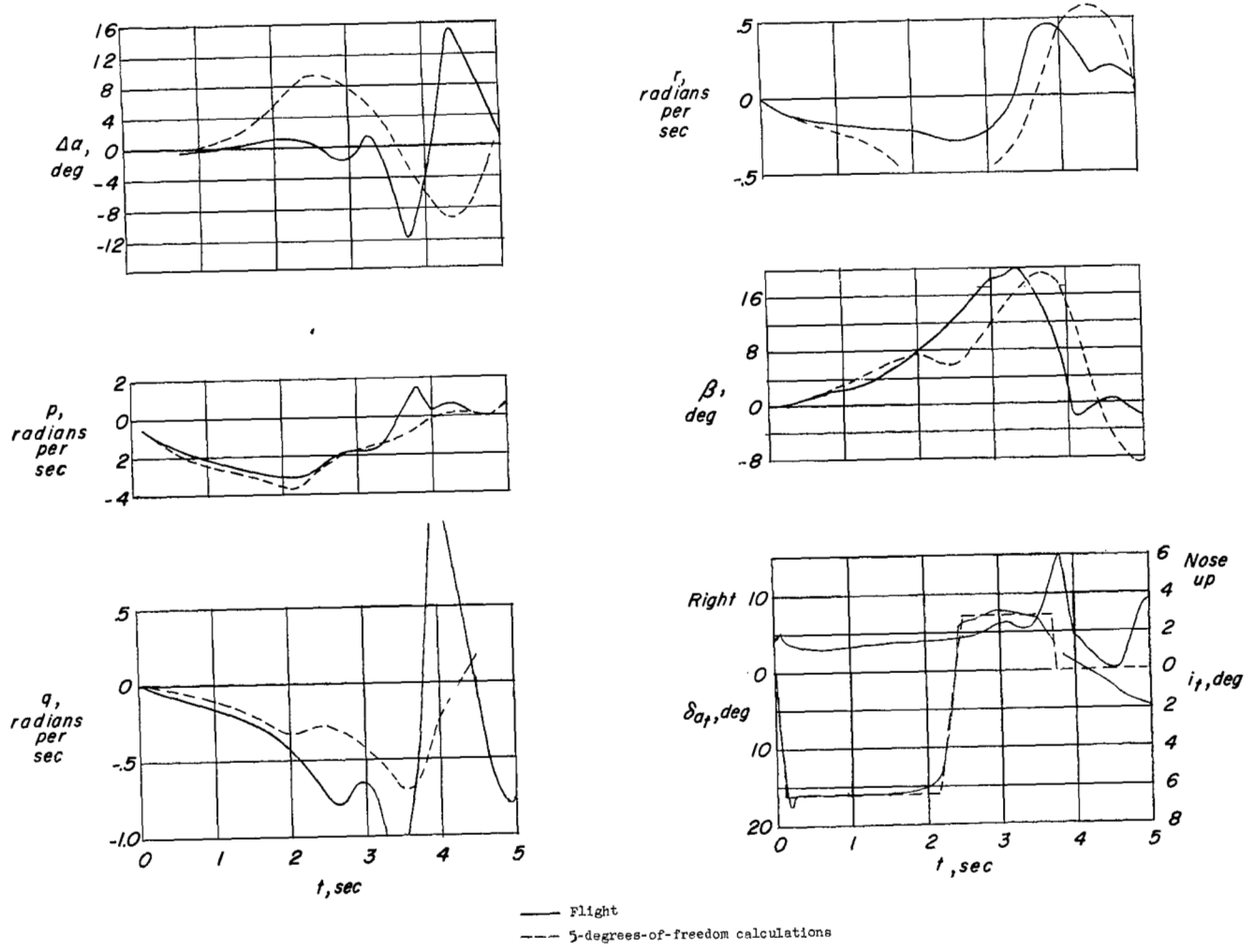


Figure 5.- Comparison of flight and calculated rolling motions of the Douglas X-3 airplane.  $M' = 1.05$ ;  $\alpha_0 = 1.8^\circ$ ; pressure altitude 30,000 feet.

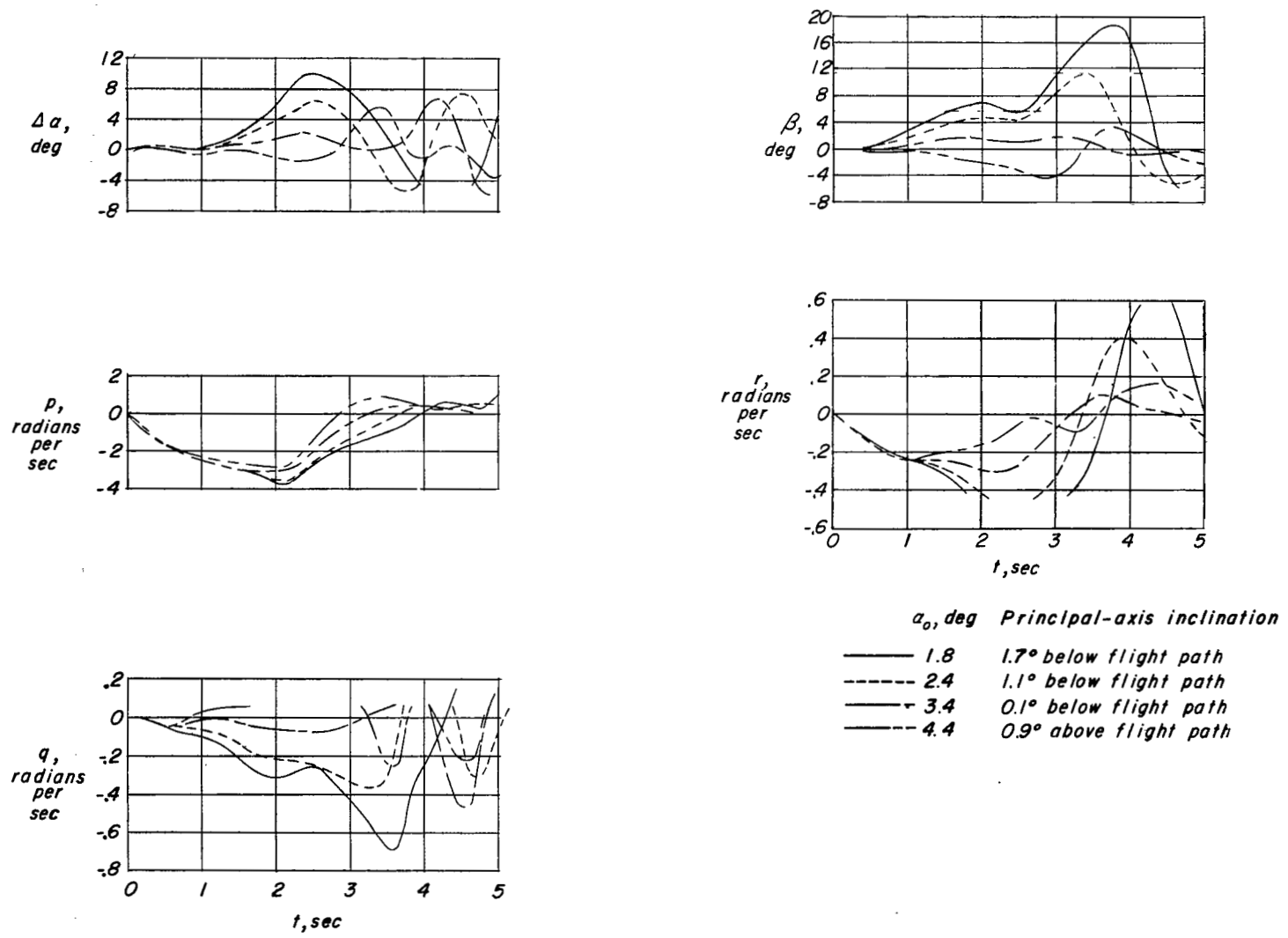


Figure 6.- Calculated effect of principal-axis inclination on the motions of the Douglas X-3 in rapid rolls.

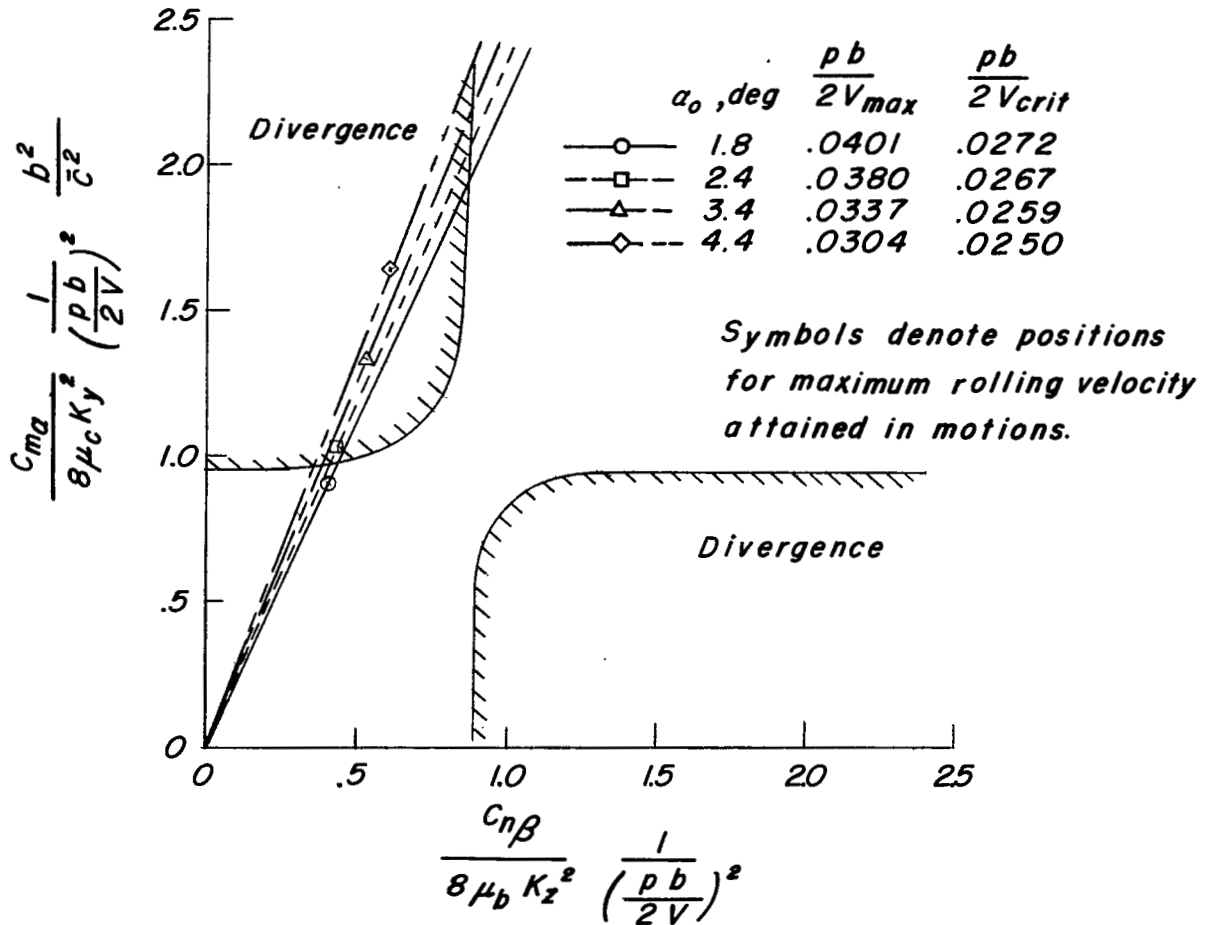


Figure 7.- Divergence boundaries based on the analysis of NACA TN 1627, showing the positions of maximum rolling conditions for various principal axes inclinations or initial angles of attack. The spread in radial lines is caused by small difference in directional stability due to angle of attack.

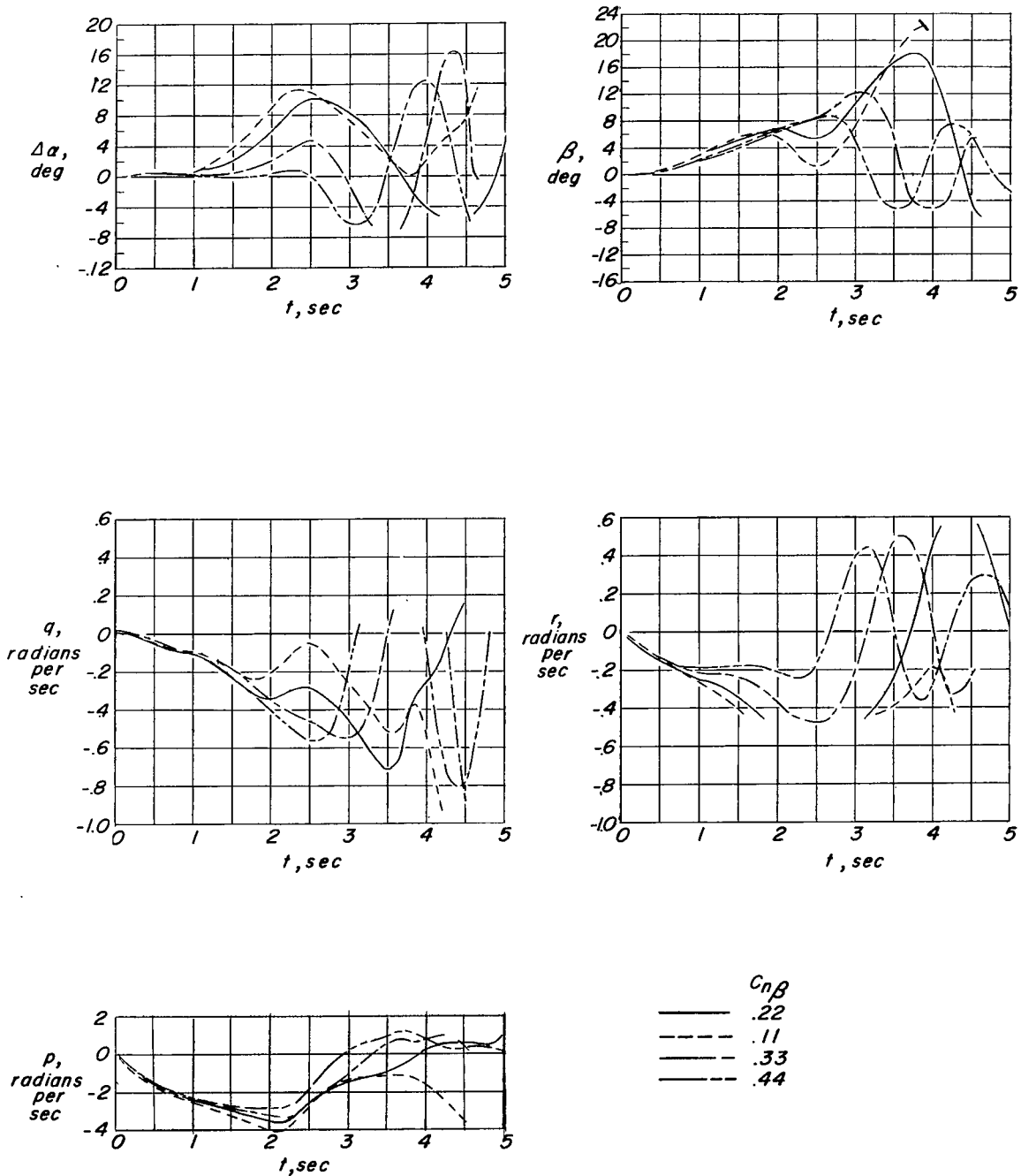


Figure 8.- Calculated effects of variations in directional stability  $C_{n\beta}$  on the motions of the Douglas X-3 airplane in rapid rolls.  $\alpha_0 = 1.8^\circ$ ;  $M' = 1.05$ .

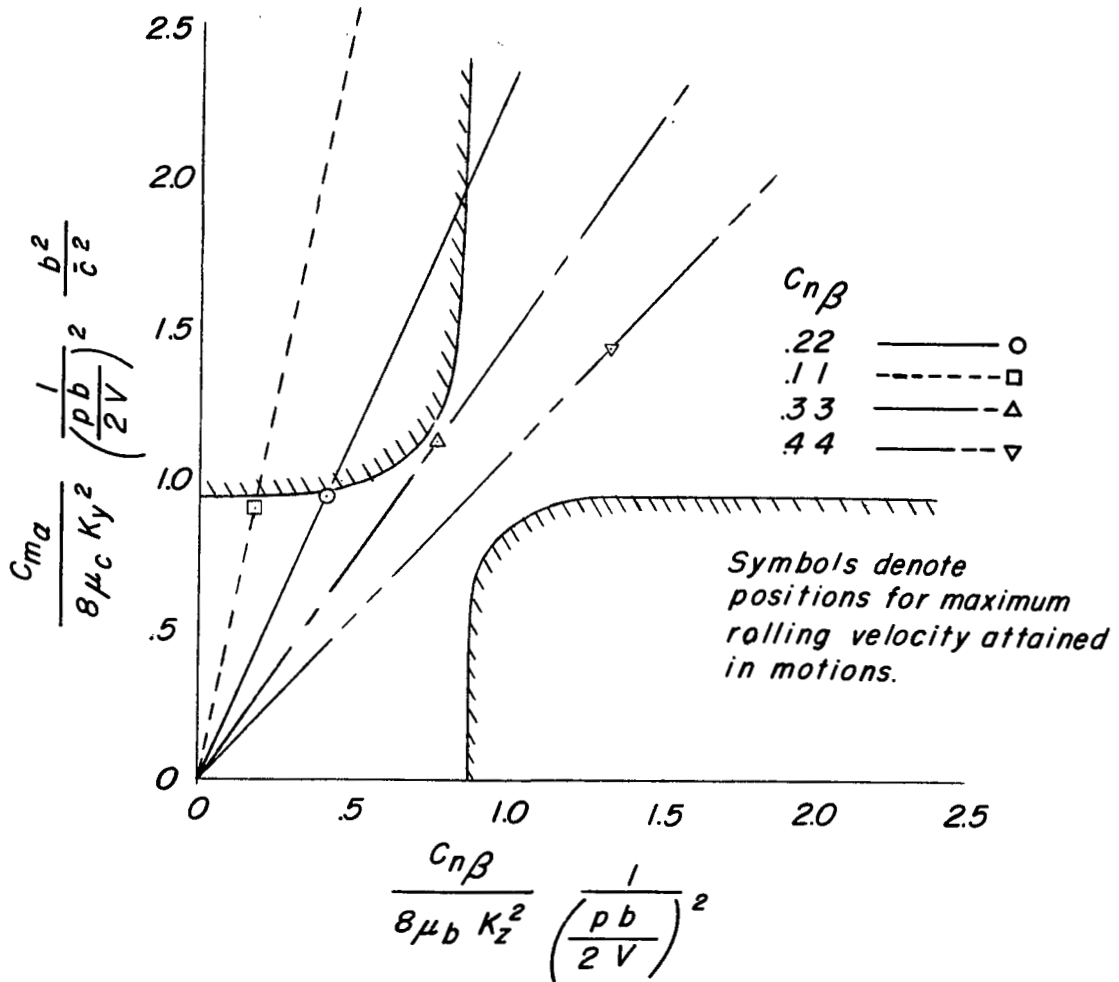
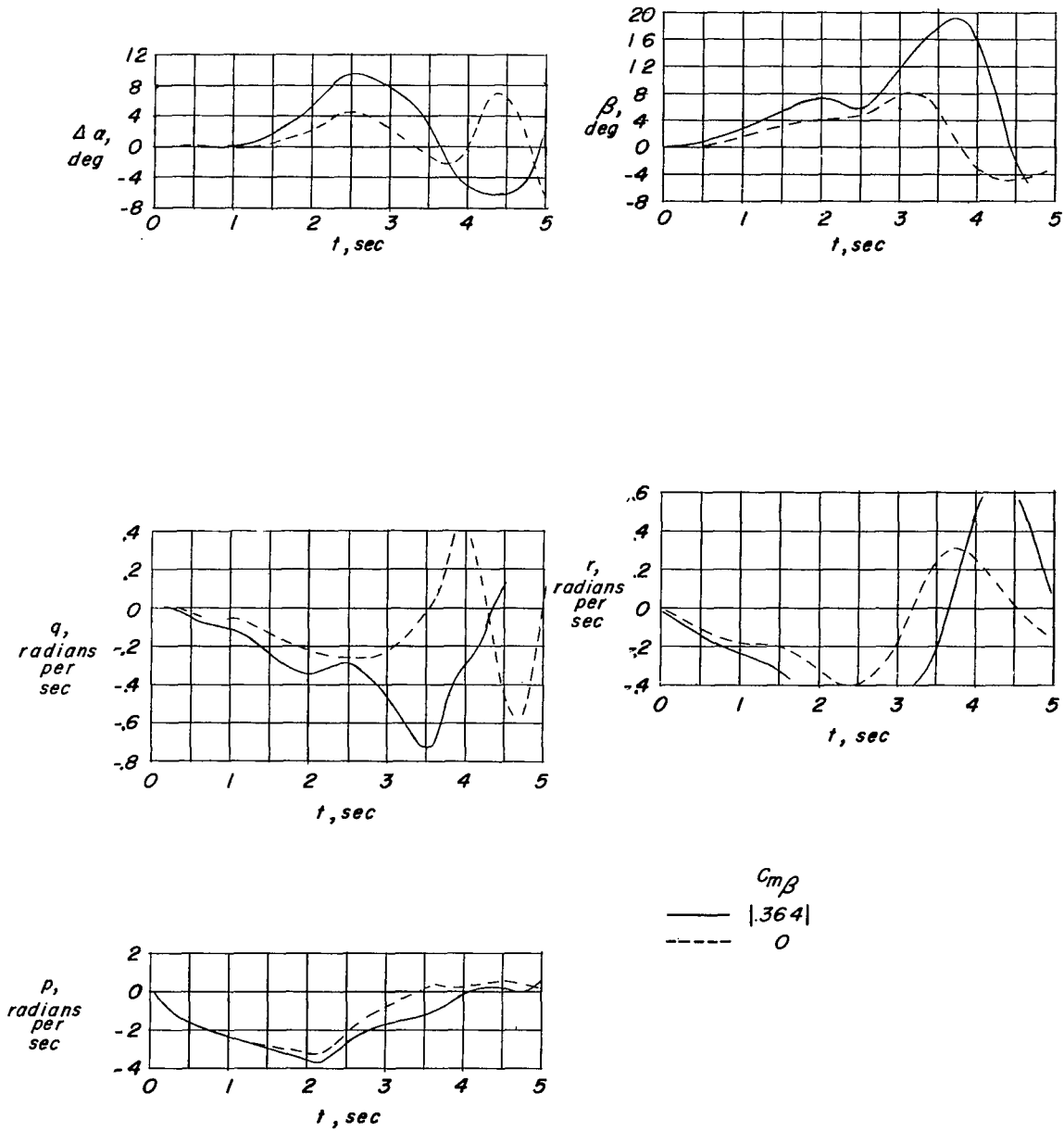


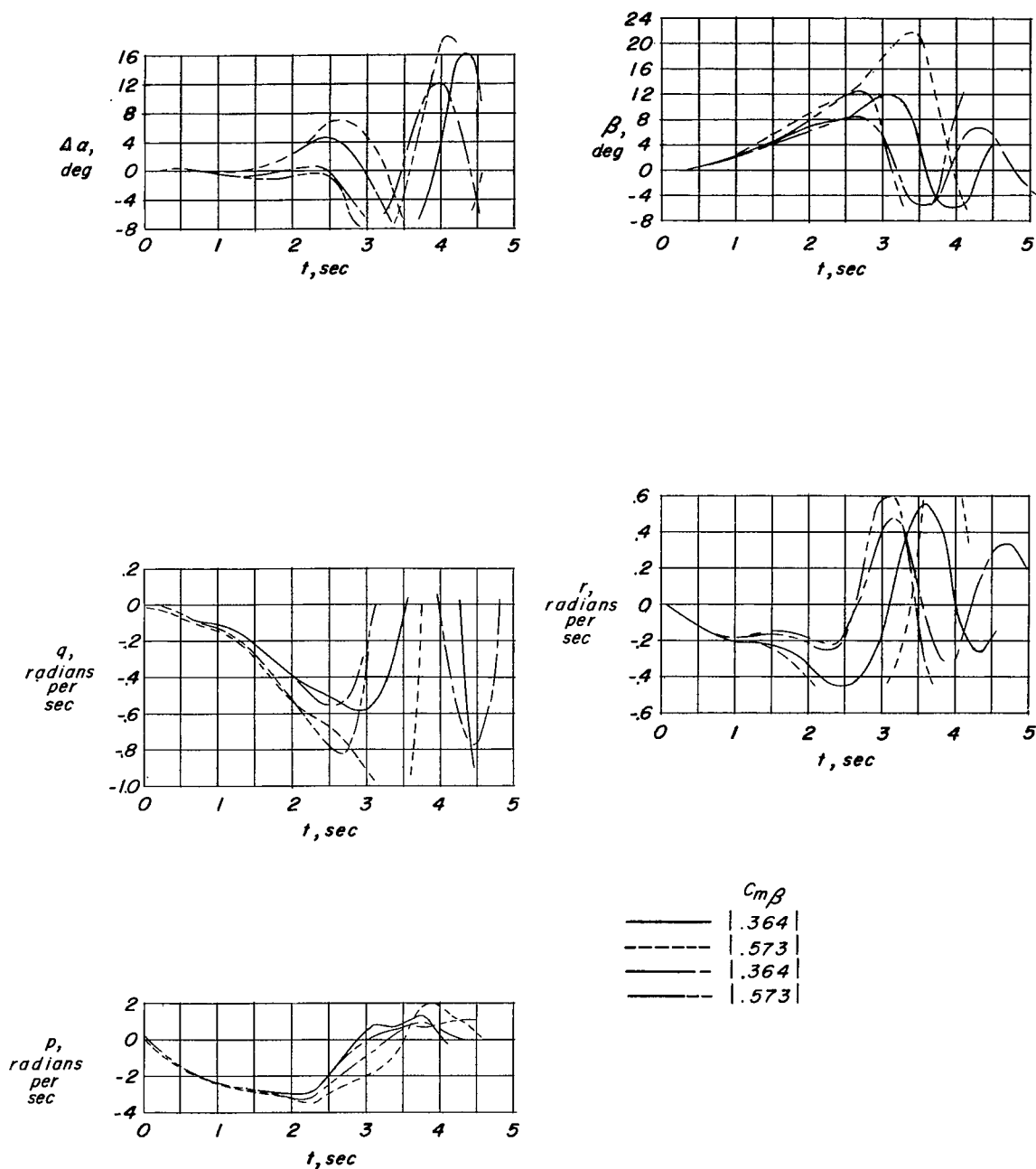
Figure 9.- Divergence boundaries, based on the analysis of NACA TN 1627, showing the effect of directional stability changes on the proximity to divergence boundaries during rolling motions.



(a)  $C_{N\beta} = 0.22$ .

Figure 10.- Calculated effect of  $C_{m\beta}$  on the motion of the Douglas X-3 airplane in rapid rolls.  $\alpha_0 = 1.8^\circ$ ;  $M' = 1.05$ .





(b)  $C_{n\beta} = 0.33$  and  $C_{n\beta} = 0.44$ .

Figure 10.- Concluded.

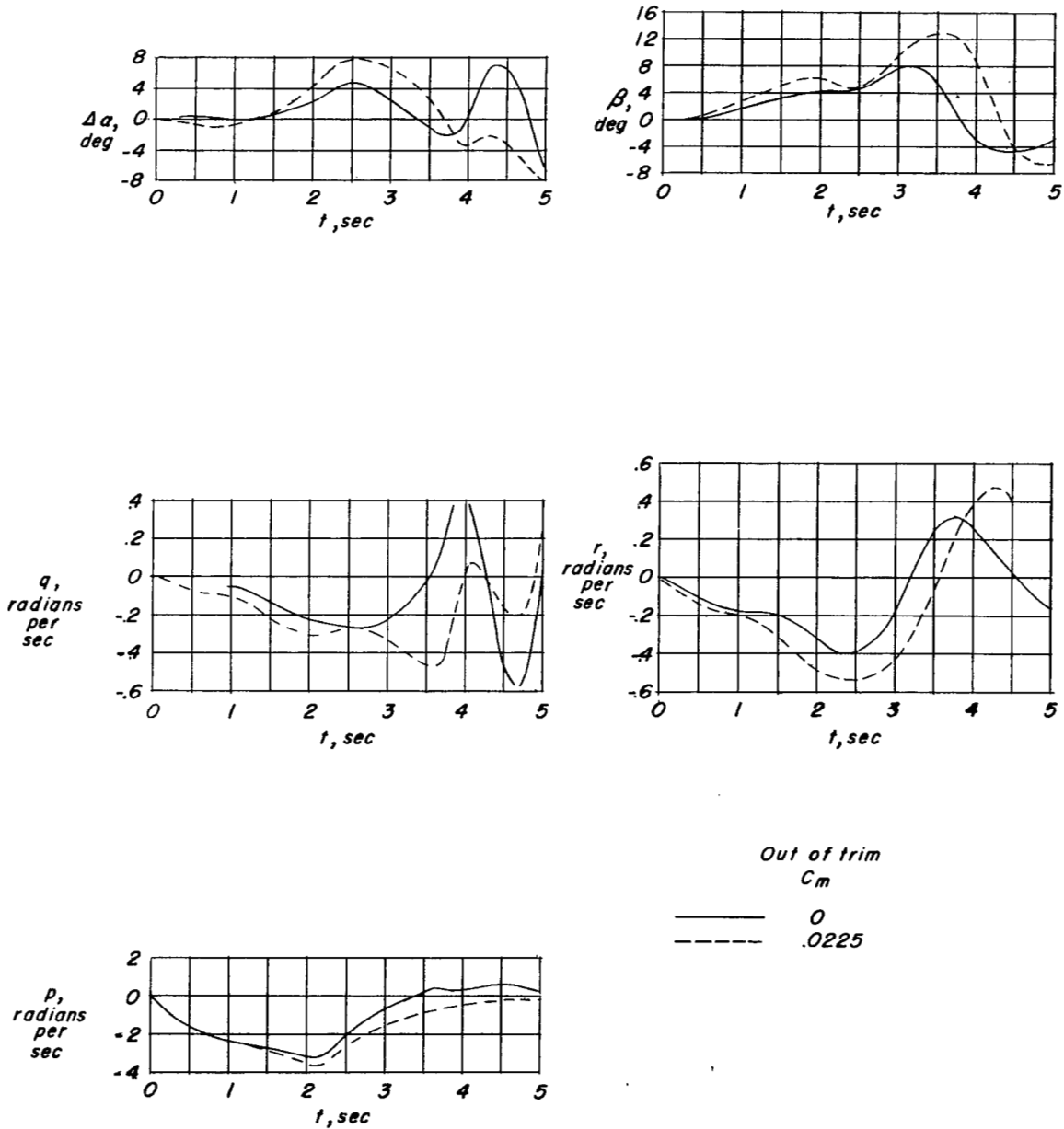
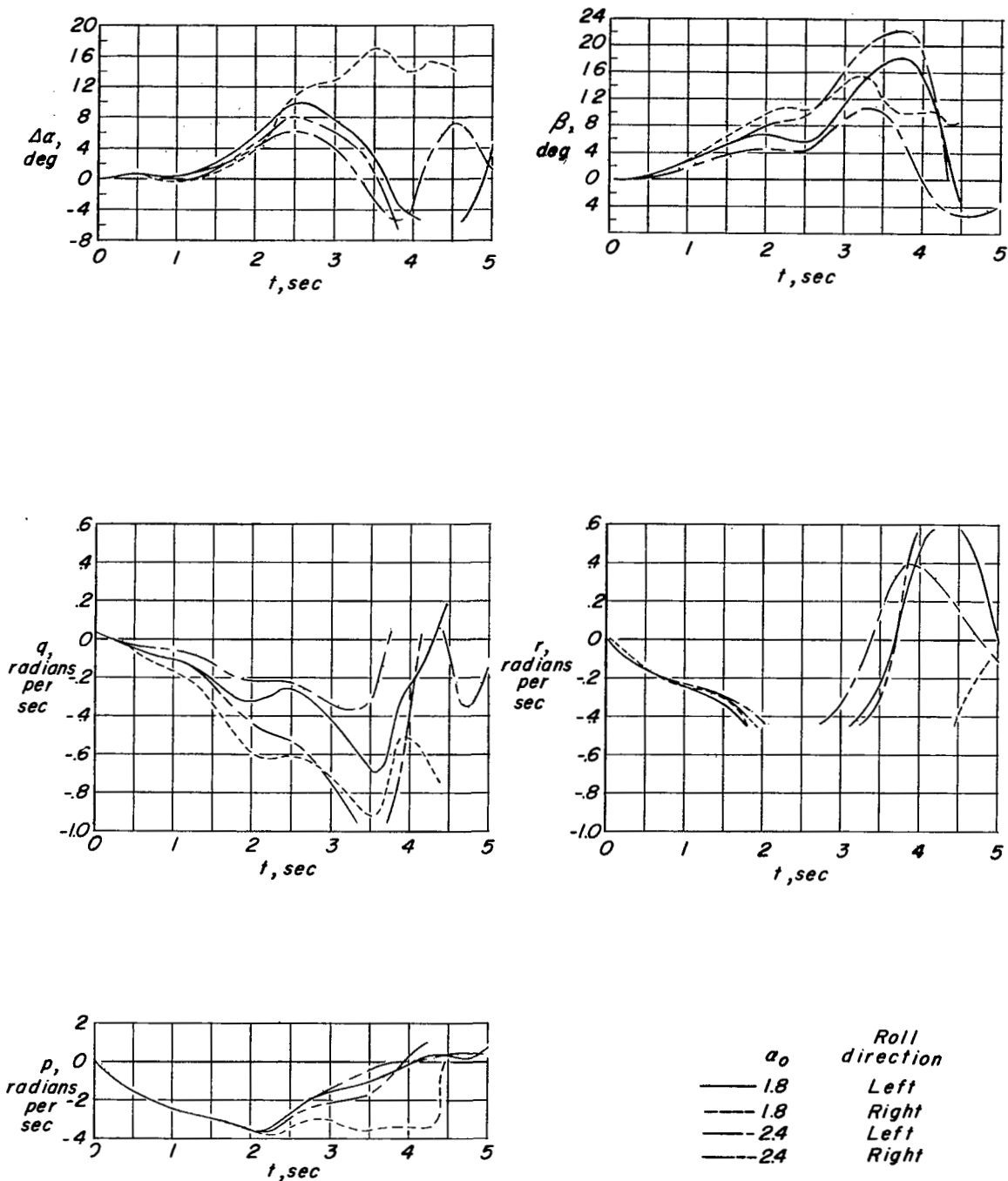
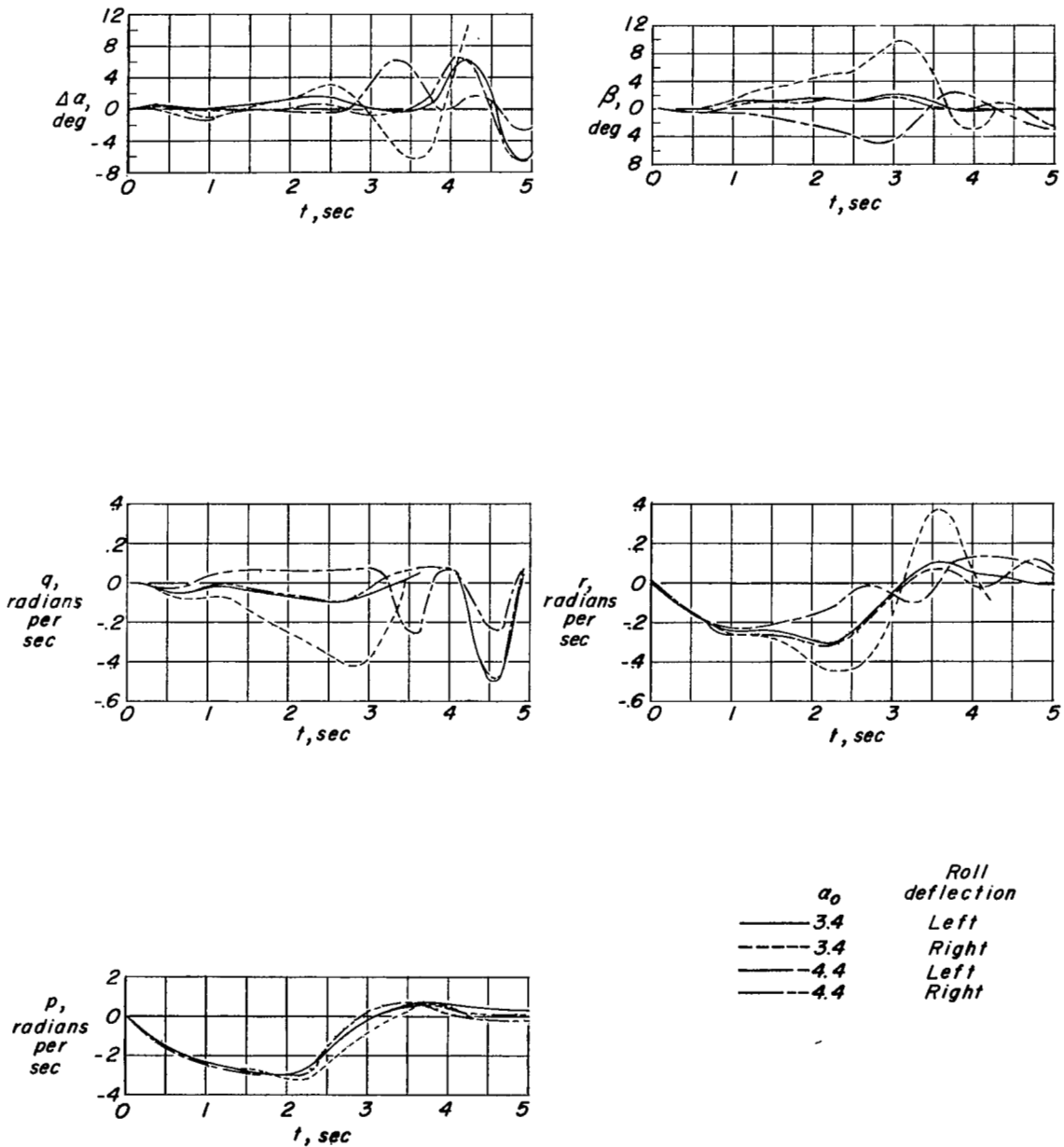


Figure 11.- Calculated effect of pitch trim change due to Mach number on the motion of the Douglas X-3 airplane in rapid rolls.  $\alpha_0 = 1.8^\circ$ ;  $M' = 1.05$ ;  $C_{m\beta} = 0$ .



(a)  $\alpha_0 = 1.8^\circ$  and  $\alpha_0 = 2.4^\circ$ .

Figure 12.- Calculated effect of roll direction on the motions of the Douglas X-3 airplane in rapid rolls. (For right rolls  $p$ ,  $\beta$ , and  $r$  are plotted with signs changed for ease of comparison.)



(b)  $\alpha_0 = 3.4^\circ$  and  $\alpha_0 = 4.4^\circ$ .

Figure 12.- Concluded.